ONE-PIXEL SHORTCUT: ON THE LEARNING PREFERENCE OF DEEP NEURAL NETWORKS

Anonymous authors
Paper under double-blind review

ABSTRACT

Unlearnable examples (ULEs) aim to protect data from unauthorized usage for training DNNs. Existing work adds ℓ_∞-bounded perturbations to the original sample so that the trained model generalizes poorly. Such perturbations, however, are easy to eliminate by, e.g., adversarial training and data augmentations. In this paper, we resolve this problem from a novel perspective by perturbing only one pixel in each image. Interestingly, such a small modification could effectively degrade model accuracy to almost an untrained counterpart. Moreover, our produced *One-Pixel Shortcut (OPS)* could not be erased by adversarial training and strong augmentations. To generate OPS, we perturb in-class images in the same pixel that, if changed to a 0 or 1, could mostly and stably deviate from all original images. Since such calculation is only based on images, OPS needs significantly less computation than the previous methods based on model training. By OPS, we introduce an unlearnable dataset called CIFAR-10-S, which is indistinguishable from CIFAR-10 by humans but induces the trained model to extremely low accuracy. Even under adversarial training, a ResNet-18 trained on CIFAR-10-S has only 10.61% accuracy, compared to 83.02% by the existing error-minimizing method.

1 INTRODUCTION

Deep neural networks (DNNs) have successfully promoted computer vision field in the past decade. As DNNs are scaling up unprecedentedly (Brock et al., 2018; Huang et al., 2019; Riquelme et al., 2021; Zhang et al., 2022), data becomes increasingly vital. For example, ImageNet (Russakovsky et al., 2015) fostered the development of AlexNet (Krizhevsky et al., 2017). Besides, people or organizations also collect online data to train DNNs, *e.g.*, IG-3.5B-17k (Mahajan et al., 2018) and JFT-300M (Sun et al., 2017). This practice, however, raises the privacy concerns of Internet users.

In this concern, researchers have made substantial efforts to protect personal data from abuse in model learning without affecting user experience (Feng et al., 2019; Huang et al., 2020a; Fowl et al., 2021; Yuan & Wu, 2021; Yu et al., 2021). Among those proposed methods, unlearnable examples (ULEs) (Huang et al., 2020a) take a great step to inject original images with protective but imperceptible perturbations from bi-level error minimization (EM). DNNs trained on ULEs generalize very poorly on normal images. However, such perturbations could be completely canceled out by adversarial training, which fails the protection, limiting the practicality of ULEs.

We view the data protection problem from the perspective of shortcut learning (Geirhos et al., 2020), which shows that DNN training is "lazy" (Chizat et al., 2019; Caron & Chrétien, 2020), *i.e.*, converges to the solution with minimum norm when optimized by gradient descent (Wilson et al., 2017; Shah et al., 2018; Zhang et al., 2021). In this case, a DNN would rely on every accessible feature to minimize the training loss, no matter whether it is semantic or not (Ilyas et al., 2019; Geirhos et al., 2018; Baker et al., 2018). Thus, DNNs tend to ignore semantic features if there are other easy-to-learn shortcuts that are sufficient for distinguishing samples in different classes.

Such shortcuts exist naturally or manually. In data collection, *e.g.*, cows may mostly appear with grasslands, misleading DNN to predict cows by large-area green, because the color is easier to learn than cow's semantic features and also sufficient to classify cows in training. Such natural shortcuts have been illustrated in detail in datasets such ImageNet-A (Hendrycks et al., 2021) and ObjectNet (Barbu et al., 2019). Besides, shortcuts could also be manually crafted (Huang et al.,

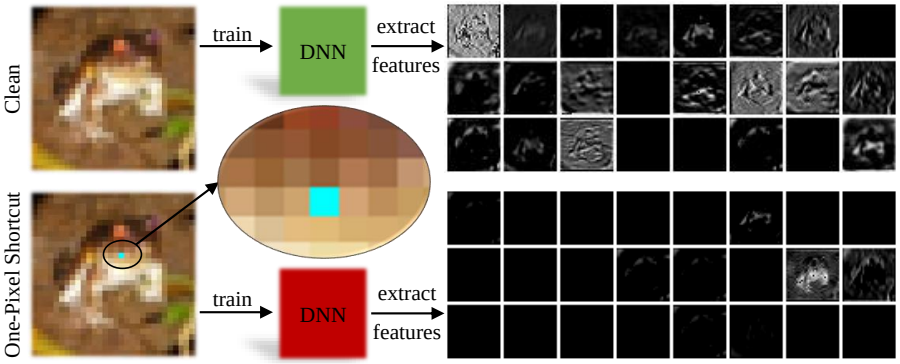

Figure 1: Effect of One-Pixel Shortcut. We visualize the features (after the first convolution) of the ResNet-18 (He et al., 2016) models trained by clean and OPS samples. Even at such a shallow layer, the DNN trained on OPS extracts much fewer semantic features and is less activated.

2020a). EM-based ULEs (Huang et al., 2020a) mislead DNNs to learn features belonging to the perturbations, which falls in the category of shortcut learning (Yu et al., 2021).

In this paper, we are surprised to find that shortcuts could be so small in the area that *it can even be simply instantiated as a single pixel*. By perturbing a pixel of each training sample, our method, namely One-Pixel Shortcut (OPS), degrades the model accuracy on clean data to almost an untrained counterpart. Moreover, our generated unbounded small noise could not be erased by adversarial training (Madry et al., 2018), which is effective in mitigating existing ULEs (Huang et al., 2020a). To make the specific pixel stand out in view of DNNs, OPS perturbs in-class images in the same pixel that, if changed to a 0 or 1, could mostly and stably deviate from all original images. Specifically, the difference between the perturbed pixel and the original one in all in-class images should be large with low variance. Since such calculation is only based on images, OPS needs significantly less computational cost than the previous methods based on model training.

We evaluate OPS and its counterparts in 6 architectures, 6 model sizes, 8 training strategies on CIFAR-10 (Krizhevsky et al., 2009) and ImageNet (Russakovsky et al., 2015) subset, and find that OPS is always superior in degrading model's testing accuracy than EM ULEs. Even under adversarial training, a ResNet-18 (He et al., 2016) trained on CIFAR-10-S has 10.61% testing accuracy, compared to 83.02% by the existing error-minimizing method. In this regard, we introduce a new unlearnable dataset named CIFAR-10-S, which combines the EM and OPS to craft stronger imperceptible ULEs. Different from the existing datasets like ImageNet-A (Hendrycks et al., 2021) or ObjectNet (Barbu et al., 2019), which place objects into special environments to remove shortcuts, CIFAR-10-S injects shortcuts to evaluate the model's resistance to them.

Contributions

- We analyze unlearnable examples from the perspective of shortcut learning, and demonstrate the DNN shortcut could be as small as a single pixel.
- We propose a novel data protection method named One-Pixel Shortcut (OPS), which perturbs in-class images in the pixel that could mostly and stably deviate from the original images. OPS is a model-free method that is significantly faster than previous work.
- We extensively evaluate OPS and find OPS outperforms baselines by a large margin in the ability to degrade accuracy, resist adversarial training, and data augmentations. Thus, we introduce CIFAR-10-S to assess the model's ability to learn semantic features.

2 Related Work

2.1 Adversarial attack and data poisoning

Adversarial examples are perturbed by small perturbations, which are indistinguishable from the original examples by humans but can make DNNs give wrong predictions (Szegedy et al., 2014).

Many different adversarial attacks are proposed in recent years. Generally, most adversarial attacks aim to perturb the whole image with a constrained intensity (usually bounded by ℓ_p norm), *e.g.*, PGD (Madry et al., 2018), C&W (Carlini & Wagner, 2017) and Autoattack (Croce & Hein, 2020). Besides, there are also other methods that only perturb a small part of an image (Croce & Hein (2019); Dong et al. (2020)) or even a single pixel (Su et al. (2019)). The existence of adversarial examples indicates that DNNs do not sufficiently learn critical semantic information as we wish, but more or less depending on some non-robust features.

Data poisoning aims to modify the training data in order to affect the performance of models. Usually, the poisoned examples are notably modified and take only a part of the whole dataset (Yang et al., 2017; Koh & Liang, 2017). But those methods cannot degrade the performance of models to a low enough level, and the poisoned examples are easily distinguishable. Recently researchers have paid great attention to imperceptible poisoning which modifies examples slightly and does not damage their semantic information (Huang et al., 2020a; Fowl et al., 2021; Huang et al., 2020b; Doan et al., 2021; Geiping et al., 2020). Fowl et al. (2021) uses adversarial perturbations which contain information of wrong labels to poison the training data, which is equivalent to random label fitting. On the contrary, Huang et al. (2020a) attack the training examples inversely, *i.e.*,using error-minimizing perturbation, to craft unlearnable examples.

2.2 Shortcut learning

Recently, researches on deep neural networks indicate that under the sufficiency of correct classification, DNNs tend to learn easier features instead of semantic features which make the object itself. To be more specific, for example, the same object in different environments will get different predictions, which means the DNN overly relies on features that do not belong to the object (Beery et al., 2018). Geirhos et al. (2020) investigate this phenomenon in different fields of deep learning and explain why shortcuts exist and how to understand them. Lapuschkin et al. (2019) also observe this problem and attribute it to the unsuitable performance evaluation metrics that we generally use. The existence of natural adversarial examples (Hendrycks et al., 2021) also indicates that DNNs do not sufficiently learn the real semantic information during training. Instead, they may learn to use the background or texture of an image to predict. Unlearnable examples (ULEs) (Huang et al., 2020a), which are manually crafted by error-minimizing noises and able to lead the models trained on them to obtain terrible generalization on test data, are believed to be some kind of shortcut that provides some textures that are easy to learn (Yu et al., 2021). Generally, if we get enough data, the interconnection of different features will be enhanced so that those shortcuts may not be sufficient for classification tasks, *i.e.*, the model will have to use more complicated composed features in order to minimize the risk. However, when the data we collect obtains some specific bias (*e.g.*, similar backgrounds), shortcut learning will not be mitigated effectively.

2.3 Data augmentation

Data augmentation aims to enhance the generalization ability of models. This is usually implemented by applying some transformations to the training data, *e.g.*, random stretching, random cropping, or color changing. Nowadays different kinds of data augmentation policies (Zhang et al., 2018; DeVries & Taylor, 2017; Cubuk et al., 2019; 2020) are proven to effectively boost the generalization ability of DNNs. Sometimes adversarial training is also regarded as a kind of data augmentation (Shorten & Khoshgoftaar, 2019; Xie et al., 2020). Dao et al. (2019) deem data augmentation as a kind of data-dependent regularization term. Since data augmentations are believed to improve the generalization ability of DNNs, we use different augmentations to evaluate the effectiveness of different data protection methods.

3 One-Pixel Shortcut

3.1 Preliminaries

Unlearnable examples (ULEs) are a data protection method created by error-minimizing (EM) noises (Huang et al., 2020a). Models trained on examples that are perturbed by those noises will get almost zero training error, but perform like random guessing on clean test data. Due to the imperceptibility

Table 1: The testing accuracy of ResNet-18 models trained on different data.

Testing / Training	Clean	EM	OPS
Clean	99.96	25.16	15.48
EM	94.00	99.99	15.54
Shuffled EM	9.97	**48.97**	10.15
OPS	99.52	25.07	99.97
Shuffled OPS	9.82	10.35	**72.43**

of the noise, this method can prevent the abuse of data by some unauthorized users who attempt to train deep models for improper purposes, without affecting normal usage. This bi-level problem can be solved by optimizing the inner minimization and the outer minimization alternately. It is proved that the perturbations belonging to the same class are well clustered and linearly separable (Yu et al., 2021). Thus, EM provides easy-to-learn features which are closely interconnected with labels.

We design a shuffling experiment to demonstrate that DNNs learn the shortcuts instead of images if trained on data that have shortcuts. Denote $\hat{\mathcal{D}} = \{(x_i + \delta_i, y_i)\}$ as the perturbed training set, where δ_i is the perturbation associated with the i-th example. After shuffling, the training set becomes $\hat{\mathcal{D}}' = \{(x_j + \delta_i, y_i)\}$. We are curious about how the DNNs trained on different data (with or without shortcuts) would predict the shuffled perturbed training set. As shown in Table 1, the DNN trained on clean data performs like a random guess on shuffled perturbed data while keeping high accuracy on unshuffled data, indicating that it successfully learns the representations from images $\{x_i\}$ rather than giving predictions according to the perturbations $\{\delta_i\}$ from EM or OPS. In contrast, the DNN trained on EM training data tends to memorize a significant proportion of perturbations, because it has 48.97% accuracy on the shuffled EM training data. Moreover, OPS training data produces a DNN with 72.43% accuracy on the shuffled set, reflecting it forcing the DNN to learn the perturbations to a greater extent. Our study illustrates the learning characteristics of DNNs trained with or without shortcuts, and also shows that OPS is a more effective shortcut than EM.

3.2 Fooling DNN training by a pixel

Following the discussion above, for the purpose of data protection, we need to craft shortcuts that are easy enough to learn and thus fool the network training. According to previous studies, shortcuts can come from background environments that naturally exist inside our datasets (Beery et al., 2018), or be manually crafted like EM (Huang et al., 2020a). Unlike those shortcuts which might occupy the whole image or a notable part, we investigate how a single pixel, which is the minimum unit of digital images, can affect the learning process of deep neural networks. Thus, we propose One-Pixel Shortcut (OPS), which modifies only a single pixel of each image. Images belonging to the same category are perturbed at the same position, which means the perturbed pixel is interconnected with the category label. Although so minuscule, it is efficient enough to fool the training of deep learning models. We use a heuristic but effective method to generate perturbations for images belonging to each category. We search the position and value of the pixel which can result in the most significant change for the whole category. Denoting $\mathcal{D}$ as the clean dataset and $\mathcal{D}_k$ as the clean subset containing all the examples of class k, the problem can be formulated as:

$$\arg\max_{\sigma_k, \xi_k} \mathbb{E}_{(x,y)\in\mathcal{D}_k} \left[\mathcal{G}_k\left(x, \sigma_k, \xi_k\right)\right] \qquad \text{s.t.} \quad \|\sigma_k\|_0 = 1, \sum_{i,j} \sigma_k(i,j) = 1, \tag{1}$$

where $\sigma_k \in \mathbb{R}^{H\times W}$ represents the perturbed position mask and $\sigma_k(i,j)$ is the element at the i-th row and j-th column, $\xi_k \in \mathbb{R}^C$ stands for the perturbed target color ($C = 3$ for RGB images), and $\mathcal{G}$ is the objective function. Since the optimization above is an NP-hard problem, we cannot solve it directly. Thus we constrain the feasible region to a limited discrete searching space, where we search the boundary value of each color channel, *i.e.*,$\xi_k \in \{0,1\}^3$, at every point of an image. Specifically, for CIFAR-10 images, the discrete searching space will contain $32 \times 32 \times 2^3 = 8192$ elements. To

ensure that the pixel is stably perturbed, we also hope that the variance of the difference between them is small. Accordingly, we design the objective function $\mathcal{G}_k$ for class k as:

$$\mathcal{G}_k = \frac{\mathbb{E}_{(x,y)\in\mathcal{D}_k}\left(\sum_{j=1}^{C}|\|x_j\cdot\sigma_k\|_F - \xi_{kj}|\right)}{\mathrm{Var}_{(x,y)\in\mathcal{D}_k}\left(\sum_{j=1}^{C}|\|x_j\cdot\sigma_k\|_F - \xi_{kj}|\right)} \tag{2}$$

where $x_i \in \mathbb{R}^{H\times W}$ denotes the i-th channel of x, and $\xi_{kj} \in \mathbb{R}$ is the i-th channel of ξ_k. After solving the position map and color, we get perturbation δ for each example (x, y) as:

$$\delta = [\xi_{y1}\sigma_y - x_1\cdot\sigma_y, \xi_{y2}\sigma_y - x_2\cdot\sigma_y, \ldots, \xi_{yC}\sigma_y - x_C\cdot\sigma_y]^\top \tag{3}$$

Details can be found in Algorithm 1. The resulting One-Pixel Shortcut is illustrated in Figure 2.

Algorithm 1 Model-Free Searching for One-Pixel Shortcut

Input: Clean dataset $\mathcal{D} = \mathcal{D}_1 \bigcup \cdots \bigcup \mathcal{D}_M$
Output: One-Pixel Shortcut dataset $\hat{\mathcal{D}} = \hat{\mathcal{D}}_1 \bigcup \cdots \bigcup \hat{\mathcal{D}}_M$

```
for k = 1, 2, 3, ..., M do
    solve Eq.1 and Eq.2 to get σ_k and ξ_k          # calculate the best perturbed point for class k
    for each x ∈ D_k do
        for i = 1, 2, 3 do
            x̂_i = x_i · (I − σ_k) + ξ_ki · σ_k      # modify the optimal pixel for every image in class k
        end for
    end for
    D̂_k = {x̂}
end for
return D̂ = D̂_1 ⋃ ··· ⋃ D̂_M
```

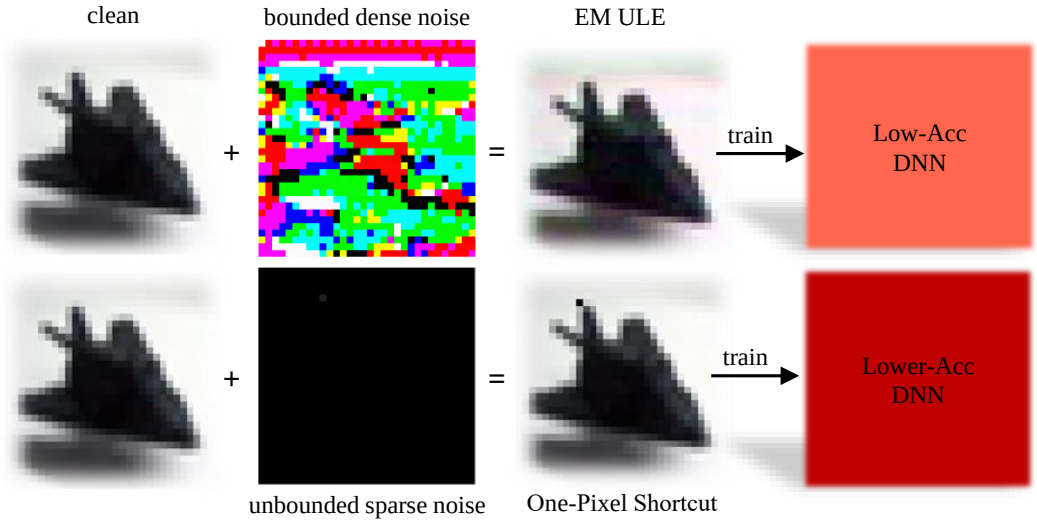

Figure 2: The effects of Error-Minimizing noise and One-Pixel Shortcut. Models trained on either EM or OPS perturbed data get abnormally low accuracy on clean test data. To ensure imperceptibility, EM adds ℓ_p bounded noise to the whole image, while OPS applies unbounded but sparse perturbation which only affects a small part of the image.

3.3 Properties of One-Pixel Shortcut

Since we all empirically believe that convolutional networks tend to capture textures (Hermann et al., 2020) or shapes (Geirhos et al., 2018; Zhang & Zhu, 2019), it is surprising that convolutional

networks can be affected so severely by just one pixel. As illustrated by Figure 1, the network indeed tends to learn those less complicated nonsemantic features brought by One-Pixel Shortcut. Besides convolutional networks, we observe that compact vision transformers (Hassani et al., 2021) are also attracted by One-Pixel Shortcut and ignore other semantic features. This indicates that shortcuts are not particularly learned by some specific architecture. We also visualize the loss landscape of ResNet-18 trained on clean CIFAR-10 data and One-Pixel Shortcut data. Illustrated as Figure 3, while trained on OPS data, the loss surface is much flatter, which means that these minima found by the network are more difficult to escape. Even if we use a ResNet-18 pretrained on clean CIFAR-10 and then fine-tune it on the OPS data, the network will still fall into this badly generalized minima.

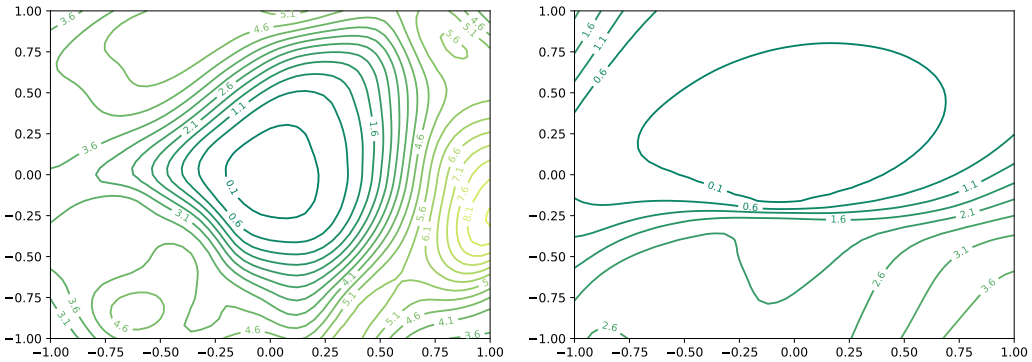

Figure 3: Loss landscape visualization (Li et al., 2018) of ResNet-18 trained on clean CIFAR-10 data and our One-Pixel Shortcut data. The landscape of THE OPS-trained model is flatter, making it minima harder to escape.

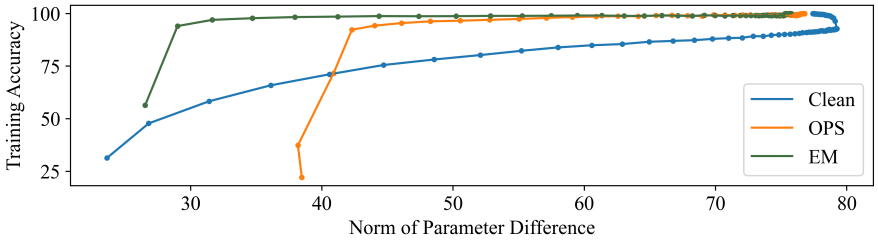

Figure 4: Training accuracy and the Frobenius norm of parameter difference (*i.e.*,$\|\theta - \theta_0\|_F$) when ResNet-18 are trained on different training data. While training on EM or OPS data, the network tends to find an optimum closer to the initialized point. This is consistent with the view of shortcut learning.

In addition, we record the trajectories of training accuracy and the Frobenius norm of parameter difference, $\|\theta - \theta_0\|_F$, which can reflect the magnitude of network parameter change. Here θ and θ_0 respectively indicate the parameters after training and at the initialized point. We draw the relation curve between training accuracy and $\|\theta - \theta_0\|_F$, which can be found in Figure 4. When training accuracy rises up to 90% for the first time, the model trained on OPS data has a much smaller $\|\theta - \theta_0\|_F$ than that trained on clean data, which indicates that the OPS-trained model gets stuck in an optimum closer to the initialization point. It has been widely known that deep models optimized by gradient descent will always converge to the solution with minimum norm (Wilson et al., 2017; Shah et al., 2018; Zhang et al., 2021). Since OPS only perturbs a single pixel, the original representations of images are not damaged, and the model trained on clean data can still keep great performance on OPS data, which indicates that the corresponding solution still exists, but due to the tendency for minimum norm solution, the well-generalized solution with lager norm is not reached. Minimum-norm solution is believed to obtain better generalization ability. Nevertheless, this argument is true only under the assumption that the training data and test data are from the exact same distribution and have the exact same features. The existence of OPS forces the model to converge to an optimum where the model generalizes well on OPS features, which are not contained in test data. From our experiment results in Table 2, OPS can degrade test accuracy to a lower level. This is because EM requires a generator

model, and thus may contain features more or less depending on it, which constrains the effectiveness of other models. On the other hand, OPS is a universal model-free method, and the shortcuts are crafted based on the inherent learning preference of DNNs.

4 EXPERIMENTS

4.1 SETTING

Our experiments are implemented on CIFAR-10 and ImageNet subset, using 4 NVIDIA RTX 2080Ti GPUs. We investigate how the One-Pixel Shortcut can affect the training of different models (including different architectures and different capacities). We evaluate our method on different models including convolutional networks (He et al., 2016; Zagoruyko & Komodakis, 2016; Huang et al., 2017) and the recently proposed compact vision transformers (Hassani et al., 2021). For all the convolutional networks, we use an SGD optimizer with a learning rate set to 0.1, momentum set to 0.9, and weight decay set to $5e-4$. For all the compact vision transformers, we use AdamW optimizer with $\beta_1 = 0.9$, $\beta_2 = 0.999$, learning rate set to $5e-4$, and weight decay set to $3e-2$. Batch size is set to 128 for all the models except WideResNet-28-10, where it is set to 64.

Table 2: Clean test accuracy on CIFAR-10 models of different architectures.

Model	Training Data		
	Clean	EM	OPS (Ours)
LeNet-5	70.27	26.98	22.19
CVT-7-4	87.46	27.60	18.21
CCT-7-3×1	88.98	27.06	17.95
DenseNet-121	94.10	23.72	11.45
ResNet-18	94.01	19.58	15.56
WideResNet-28-10	96.08	23.96	12.76

Besides, We also try different training strategies including adversarial training (Madry et al., 2018) and different data augmentations (Mixup (Zhang et al., 2018), Cutout (DeVries & Taylor, 2017) and RandAugment (Cubuk et al., 2020)). For adversarial training, we use a 10-step PGD attack, setting step size to $2/255$ and ℓ_∞ bound to $8/255$. For Mixup, Cutout, and RandAugment, we use the default settings from their original papers. All the models are trained for 200 epochs with a multi-step learning rate schedule, and the training accuracy of each model is guaranteed to reach near 100%.

We additionally tested our method on the ImageNet subset (the first 100 classes). We center-crop all the images to 224×224, and train common DNNs with results in Table 4. We adopt an initial learning rate of 0.1 with a multi-step learning rate scheduler and train models for 200 epochs. Our One-Pixel Shortcut can still be effective in protecting large-scale datasets. The networks trained on OPS data will get much lower clean test accuracy than those trained on clean data.

Table 3: WideResNets of different capacities trained on One-Pixel Shortcut data. Test Acc. stands for accuracy on the clean CIFAR-10 testset.

	WRN-28-1	WRN-28-2	WRN-28-4	WRN-28-8	WRN-28-16	WRN-28-20
Size	0.37M	1.47M	5.85M	23.36M	93.35M	145.84M
Test Acc.	21.20	14.74	21.75	18.01	15.36	18.04

4.2 EFFECTIVENESS ON DIFFERENT MODELS

We train different convolutional networks and vision transformers on the One-Pixel Shortcut CIFAR-10 training set, and evaluate their performance on the unmodified CIFAR-10 test set. Details are shown in Table 2. Every model reaches a very high training accuracy after only several epochs, which is much faster than training on clean data. Meanwhile, they all get really low test accuracy (about 15%) on clean test data, indicating that they do not generalize at all. Although the perturbed image looks virtually the same as the original image, and all the models get near 100% training accuracy quickly, they do not capture any semantic information but just the pixels

Table 4: Clean test accuracy on ImageNet models of different architectures.

Model	Training Data	
	Clean	OPS (Ours)
ResNet-18	76.18	9.68
ResNet-50	64.26	10.38
DenseNet-121	75.14	11.48

we modify in the images. We also train models on EM training set, which is generated by a ResNet-18 using the official implementation of Huang et al. (2020a). The ℓ_∞ bound of EM noises is set to $8/255$. The generation of OPS costs only about 30 seconds, which is much faster than EM costing about half an hour. For different networks, OPS can degrade their test accuracy to a lower level than EM. EM works the best on ResNet-18 (19.58% test accuracy), which has the same architecture as the generator. On other models, their get higher test accuracy than ResNet-18. Meanwhile, since OPS is a model-free method that takes advantage of the natural learning preference of neural networks, its transferability is better across different models. Besides different architectures, we also explore the impact on models with the same architecture but different capacities. We trained several WideResNets (Zagoruyko & Komodakis, 2016) with different sizes. The experiment results can be found in Table 3. We observe that overparameterization, which is generally believed to enhance the ability to capture complicated features, does not circumvent the shortcut features.

Moreover, we observe that vision transformers are easily affected by manually crafted shortcuts, even though it is believed that their self-attention mechanism makes them less sensitive to data distribution shifts (Shao et al., 2021; Bhojanapalli et al., 2021). For CCT-7-3$\times$1 and CVT-7-4 (Hassani et al., 2021), EM and OPS can degrade their test accuracy below 30% and 20%. This indicates that vision transformers may not generalize on out-of-distributions data as well as our expectations. If the training data is largely biased, *i.e.*, has notable shortcuts, and vision transformers will not perform much better than convolutional networks.

Table 5: Effectiveness of One-Pixel Shortcut & Error-Minimizing on ResNet-18 under different training strategies. Here ℓ_∞ AT stands for adversarial training with bound $8/255$.

Training Strategy	Training Data			
	Clean	EM	OPS	CIFAR-10-S
Standard	94.01	19.58	15.56	16.67
Mixup	94.75	38.18	33.13	23.23
Cutout	94.77	25.83	61.68	24.38
RandAugment	94.91	51.66	71.18	39.62
RandAugment + Cutout	94.86	36.26	79.70	33.85
ℓ_∞ AT	82.72	83.02	11.08	10.61
ℓ_∞ AT + Mixup	87.90	86.71	10.97	13.77
ℓ_∞ AT + Cutout	84.58	84.24	24.60	23.78
ℓ_∞ AT + RandAugment	85.50	85.06	44.86	46.23

4.3 Effectiveness under different training strategies

To evaluate the effectiveness of OPS under different training strategies, we train models on OPS perturbed data using adversarial training and different data augmentations such as Mixup (Zhang et al., 2018), Cutout (DeVries & Taylor, 2017) and RandAugment (Cubuk et al., 2020). Simple augmentations like random crop and flip are used by default in standard training. Models are also trained on EM perturbed data. As shown in Table 5, we can observe that both EM and OPS have a good performance on data protection, which degrade test accuracy to 19.58% and 15.56%. As mentioned in previous works (Huang et al., 2020a; Fu et al., 2021), EM can not work so effectively under adversarial training, and the model can reach an even higher accuracy than adversarially trained on clean data. Meanwhile, OPS can still keep effective under adversarial training. However, when it comes to data augmentation, EM seems more impervious, while OPS is more sensitive, especially to Cutout and RandAugment. This is due to the fact that EM injects global noises into images, while OPS only modifies a single pixel, which is equivalent to adding a very local perturbation. Adversarial training, which can be regarded as a kind of global augmentation, is able to attenuate the dependence on global shortcuts. On the other hand, local data augmentations like Cutout make models less sensitive to local shortcuts.

Naturally, for the purpose of complementing each other, we can combine EM and our proposed OPS together to craft a kind of ensemble shortcut. Since OPS only modified a single pixel, after being applied to EM perturbed images, the imperceptibility can still be guaranteed. We evaluate the effectiveness of this ensemble method under different training strategies and find that it can always

keep effective. Even if we use adversarial training and strong data augmentation like RandAugment, it is still able to degrade test accuracy to a relatively low level. Based on this property, we introduce CIFAR-10-S, where all the images are perturbed by the EM-OPS-composed noises. It can serve as a new benchmark to evaluate the ability to learn critical information under the disturbance of composed non-semantic representations.

We also extend our method to multi-pixel scenarios. According to Table 6, as the number of perturbed pixels increases, the test accuracy can be degraded to a lower level. Nevertheless, the more pixels are perturbed, the imperceptibility gets weaker, as illustrated in Figure 5. From our experiment on ResNet-18, 3-Pixel Shortcut can easily degrade the test accuracy to 9.74%. Moreover, more perturbed pixels alleviate the sensitivity to different data augmentations. For RandAugment, one more perturbed pixel can degrade the test accuracy to 46.45%, which is much lower than 71.18% of OPS.

Table 6: Effectiveness of Multi-Pixel Shortcut on ResNet-18 under different training strategies

Training Strategy	Number of Perturbed Pixels				
	0	1	2	3	4
Standard	94.01	15.56	15.24	9.74	9.71
Mixup	94.75	33.13	9.99	9.94	10.02
Cutout	94.77	61.68	39.99	25.42	20.15
RandAugment	94.91	71.18	46.45	34.66	33.51

0 Pixel (Clean) 1 Pixel 2 Pixels 3 Pixels 4 Pixels

Figure 5: Multi-Pixel Shortcut examples. More perturbed pixels lead to lower imperceptibility.

5 Discussion and Conclusion

In this paper, we study the mechanism of recently proposed unlearnable examples (ULEs) which use error-minimizing (EM) noises. We figure out that instead of semantic features contained by images themselves, features from EM noises are mainly learned by DNNs after training. These kinds of easy-to-learn representations work as shortcuts, which could naturally exist or be manually crafted. Since DNNs optimized by gradient descent always find the solution with the minimum norm, shortcuts take precedence over those semantic features during training.

We find that shortcuts can be as small as even a single pixel. Thus, we propose One-Pixel Shortcut (OPS), which is an imperceivable and effective data protection method. OPS does not require a generator model and therefore needs very little computational cost and has better transferability between different models. Besides, OPS is less sensitive to adversarial training compared to EM ULEs. We investigate the effectiveness of OPS and EM under different training strategies. We find that EM and OPS have their respective advantages and disadvantages. While EM cannot keep effective under global data augmentations like adversarial training, OPS is sensitive to local data augmentations like Cutout. Based on our investigation, we combine EM and OPS together to craft a kind of stronger unlearnable examples, which can still keep imperceptible but more impervious, and consequently introduce CIFAR-10-S, which can be a new benchmark. Besides, we have also discussed our method in multi-pixel scenarios.

There are still questions that need to be discussed in the future. Besides shortcuts that are crafted deliberately for the purpose of data protection, there are also shortcuts that naturally exist due to the inevitable bias during data collection. They can be the crux of network generalization on unseen data. How to identify and avoid them (*e.g.*, design data-dependent augmentation) is a challenging problem. We believe our work will shed light on the important impacts of shortcuts, and provide inspiration to harness them for more practical applications.

REFERENCES

Nicholas Baker, Hongjing Lu, Gennady Erlikhman, and Philip J Kellman. Deep convolutional networks do not classify based on global object shape. *PLoS computational biology*, 14(12): e1006613, 2018.

Andrei Barbu, David Mayo, Julian Alverio, William Luo, Christopher Wang, Dan Gutfreund, Josh Tenenbaum, and Boris Katz. Objectnet: A large-scale bias-controlled dataset for pushing the limits of object recognition models. *Advances in Neural Information Processing Systems*, 32, 2019.

Sara Beery, Grant Van Horn, and Pietro Perona. Recognition in terra incognita. In *Proceedings of the European Conference on Computer Vision*, pp. 456–473, 2018.

Srinadh Bhojanapalli, Ayan Chakrabarti, Daniel Glasner, Daliang Li, Thomas Unterthiner, and Andreas Veit. Understanding robustness of transformers for image classification. In *Proceedings of the IEEE/CVF International Conference on Computer Vision*, pp. 10231–10241, 2021.

Andrew Brock, Jeff Donahue, and Karen Simonyan. Large scale gan training for high fidelity natural image synthesis. In *International Conference on Learning Representations*, 2018.

Nicholas Carlini and David Wagner. Towards evaluating the robustness of neural networks. In *IEEE Symposium on Security and Privacy*, pp. 39–57. IEEE, 2017.

Emmanuel Caron and Stéphane Chrétien. A finite sample analysis of the benign overfitting phenomenon for ridge function estimation. *arXiv preprint arXiv:2007.12882*, 2020.

Lenaic Chizat, Edouard Oyallon, and Francis Bach. On lazy training in differentiable programming. *Advances in Neural Information Processing Systems*, 32, 2019.

Francesco Croce and Matthias Hein. Sparse and imperceivable adversarial attacks. In *Proceedings of the IEEE/CVF International Conference on Computer Vision*, pp. 4724–4732, 2019.

Francesco Croce and Matthias Hein. Reliable evaluation of adversarial robustness with an ensemble of diverse parameter-free attacks. In *International Conference on Machine Learning*, pp. 2206–2216. PMLR, 2020.

Ekin D Cubuk, Barret Zoph, Dandelion Mane, Vijay Vasudevan, and Quoc V Le. Autoaugment: Learning augmentation strategies from data. In *Proceedings of the IEEE/CVF Conference on Computer Vision and Pattern Recognition*, pp. 113–123, 2019.

Ekin D Cubuk, Barret Zoph, Jonathon Shlens, and Quoc V Le. Randaugment: Practical automated data augmentation with a reduced search space. In *Proceedings of the IEEE/CVF Conference on Computer Vision and Pattern Recognition Workshops*, pp. 702–703, 2020.

Tri Dao, Albert Gu, Alexander Ratner, Virginia Smith, Chris De Sa, and Christopher Ré. A kernel theory of modern data augmentation. In *International Conference on Machine Learning*, pp. 1528–1537. PMLR, 2019.

Terrance DeVries and Graham W Taylor. Improved regularization of convolutional neural networks with cutout. *arXiv preprint arXiv:1708.04552*, 2017.

Khoa Doan, Yingjie Lao, Weijie Zhao, and Ping Li. Lira: Learnable, imperceptible and robust backdoor attacks. In *Proceedings of the IEEE/CVF International Conference on Computer Vision*, pp. 11966–11976, 2021.

Xiaoyi Dong, Dongdong Chen, Jianmin Bao, Chuan Qin, Lu Yuan, Weiming Zhang, Nenghai Yu, and Dong Chen. Greedyfool: Distortion-aware sparse adversarial attack. *Advances in Neural Information Processing Systems*, 33:11226–11236, 2020.

Ji Feng, Qi-Zhi Cai, and Zhi-Hua Zhou. Learning to confuse: generating training time adversarial data with auto-encoder. *Advances in Neural Information Processing Systems*, 32, 2019.

Liam H Fowl, Micah Goldblum, Ping-yeh Chiang, Jonas Geiping, Wojciech Czaja, and Tom Goldstein. Adversarial examples make strong poisons. In *Advances in Neural Information Processing Systems*, 2021.

Shaopeng Fu, Fengxiang He, Yang Liu, Li Shen, and Dacheng Tao. Robust unlearnable examples: Protecting data privacy against adversarial learning. In *International Conference on Learning Representations*, 2021.

Jonas Geiping, Liam H Fowl, W Ronny Huang, Wojciech Czaja, Gavin Taylor, Michael Moeller, and Tom Goldstein. Witches' brew: Industrial scale data poisoning via gradient matching. In *International Conference on Learning Representations*, 2020.

Robert Geirhos, Patricia Rubisch, Claudio Michaelis, Matthias Bethge, Felix A Wichmann, and Wieland Brendel. Imagenet-trained cnns are biased towards texture; increasing shape bias improves accuracy and robustness. In *International Conference on Learning Representations*, 2018.

Robert Geirhos, Jörn-Henrik Jacobsen, Claudio Michaelis, Richard Zemel, Wieland Brendel, Matthias Bethge, and Felix A Wichmann. Shortcut learning in deep neural networks. *Nature Machine Intelligence*, 2(11):665–673, 2020.

Ali Hassani, Steven Walton, Nikhil Shah, Abulikemu Abuduweili, Jiachen Li, and Humphrey Shi. Escaping the big data paradigm with compact transformers. *arXiv preprint arXiv:2104.05704*, 2021.

Kaiming He, Xiangyu Zhang, Shaoqing Ren, and Jian Sun. Deep residual learning for image recognition. In *Proceedings of the IEEE/CVF Conference on Computer Vision and Pattern Recognition*, pp. 770–778, 2016.

Dan Hendrycks, Kevin Zhao, Steven Basart, Jacob Steinhardt, and Dawn Song. Natural adversarial examples. In *Proceedings of the IEEE/CVF Conference on Computer Vision and Pattern Recognition*, pp. 15262–15271, 2021.

Katherine Hermann, Ting Chen, and Simon Kornblith. The origins and prevalence of texture bias in convolutional neural networks. *Advances in Neural Information Processing Systems*, 33: 19000–19015, 2020.

Gao Huang, Zhuang Liu, Laurens Van Der Maaten, and Kilian Q Weinberger. Densely connected convolutional networks. In *Proceedings of the IEEE/CVF Conference on Computer Vision and Pattern Recognition*, pp. 4700–4708, 2017.

Hanxun Huang, Xingjun Ma, Sarah Monazam Erfani, James Bailey, and Yisen Wang. Unlearnable examples: Making personal data unexploitable. In *International Conference on Learning Representations*, 2020a.

W Ronny Huang, Jonas Geiping, Liam Fowl, Gavin Taylor, and Tom Goldstein. Metapoison: Practical general-purpose clean-label data poisoning. *Advances in Neural Information Processing Systems*, 33:12080–12091, 2020b.

Yanping Huang, Youlong Cheng, Ankur Bapna, Orhan Firat, Dehao Chen, Mia Chen, HyoukJoong Lee, Jiquan Ngiam, Quoc V Le, Yonghui Wu, et al. Gpipe: Efficient training of giant neural networks using pipeline parallelism. *Advances in Neural Information Processing Systems*, 32, 2019.

Andrew Ilyas, Shibani Santurkar, Dimitris Tsipras, Logan Engstrom, Brandon Tran, and Aleksander Madry. Adversarial examples are not bugs, they are features. *Advances in Neural Information Processing Systems*, 32, 2019.

Pang Wei Koh and Percy Liang. Understanding black-box predictions via influence functions. In *International Conference on Machine Learning*, pp. 1885–1894. PMLR, 2017.

Alex Krizhevsky, Geoffrey Hinton, et al. Learning multiple layers of features from tiny images. 2009.

Alex Krizhevsky, Ilya Sutskever, and Geoffrey E Hinton. Imagenet classification with deep convolutional neural networks. *Communications of the ACM*, 60(6):84–90, 2017.

Sebastian Lapuschkin, Stephan Wäldchen, Alexander Binder, Grégoire Montavon, Wojciech Samek, and Klaus-Robert Müller. Unmasking clever hans predictors and assessing what machines really learn. *Nature communications*, 10(1):1–8, 2019.

Hao Li, Zheng Xu, Gavin Taylor, Christoph Studer, and Tom Goldstein. Visualizing the loss landscape of neural nets. *Advances in Neural Information Processing Systems*, 31, 2018.

Aleksander Madry, Aleksandar Makelov, Ludwig Schmidt, Dimitris Tsipras, and Adrian Vladu. Towards deep learning models resistant to adversarial attacks. In *International Conference on Learning Representations*, 2018.

Dhruv Mahajan, Ross Girshick, Vignesh Ramanathan, Kaiming He, Manohar Paluri, Yixuan Li, Ashwin Bharambe, and Laurens Van Der Maaten. Exploring the limits of weakly supervised pretraining. In *Proceedings of the European Conference on Computer Vision*, pp. 181–196, 2018.

Carlos Riquelme, Joan Puigcerver, Basil Mustafa, Maxim Neumann, Rodolphe Jenatton, André Susano Pinto, Daniel Keysers, and Neil Houlsby. Scaling vision with sparse mixture of experts. *Advances in Neural Information Processing Systems*, 34, 2021.

Olga Russakovsky, Jia Deng, Hao Su, Jonathan Krause, Sanjeev Satheesh, Sean Ma, Zhiheng Huang, Andrej Karpathy, Aditya Khosla, Michael Bernstein, et al. Imagenet large scale visual recognition challenge. *International Journal of Computer Vision*, 115(3):211–252, 2015.

Vatsal Shah, Anastasios Kyrillidis, and Sujay Sanghavi. Minimum norm solutions do not always generalize well for over-parameterized problems. *stat*, 1050:16, 2018.

Rulin Shao, Zhouxing Shi, Jinfeng Yi, Pin-Yu Chen, and Cho-Jui Hsieh. On the adversarial robustness of visual transformers. *arXiv e-prints*, pp. arXiv–2103, 2021.

Connor Shorten and Taghi M Khoshgoftaar. A survey on image data augmentation for deep learning. *Journal of Big Data*, 6(1):1–48, 2019.

Jiawei Su, Danilo Vasconcellos Vargas, and Kouichi Sakurai. One pixel attack for fooling deep neural networks. *IEEE Transactions on Evolutionary Computation*, 23(5):828–841, 2019.

Chen Sun, Abhinav Shrivastava, Saurabh Singh, and Abhinav Gupta. Revisiting unreasonable effectiveness of data in deep learning era. In *Proceedings of the IEEE/CVF International Conference on Computer Vision*, pp. 843–852, 2017.

Christian Szegedy, Wojciech Zaremba, Ilya Sutskever, Joan Bruna, Dumitru Erhan, Ian Goodfellow, and Rob Fergus. Intriguing properties of neural networks. In *International Conference on Learning Representations*, 2014.

Ashia C Wilson, Rebecca Roelofs, Mitchell Stern, Nati Srebro, and Benjamin Recht. The marginal value of adaptive gradient methods in machine learning. *Advances in Neural Information Processing Systems*, 30, 2017.

Cihang Xie, Mingxing Tan, Boqing Gong, Jiang Wang, Alan L Yuille, and Quoc V Le. Adversarial examples improve image recognition. In *Proceedings of the IEEE/CVF Conference on Computer Vision and Pattern Recognition*, pp. 819–828, 2020.

Chaofei Yang, Qing Wu, Hai Li, and Yiran Chen. Generative poisoning attack method against neural networks. *arXiv preprint arXiv:1703.01340*, 2017.

Da Yu, Huishuai Zhang, Wei Chen, Jian Yin, and Tie-Yan Liu. Indiscriminate poisoning attacks are shortcuts. *arXiv preprint arXiv:2111.00898*, 2021.

Chia-Hung Yuan and Shan-Hung Wu. Neural tangent generalization attacks. In *International Conference on Machine Learning*, pp. 12230–12240. PMLR, 2021.

Sergey Zagoruyko and Nikos Komodakis. Wide residual networks. In *British Machine Vision Conference 2016*. British Machine Vision Association, 2016.

Chiyuan Zhang, Samy Bengio, Moritz Hardt, Benjamin Recht, and Oriol Vinyals. Understanding deep learning (still) requires rethinking generalization. *Communications of the ACM*, 64(3):107–115, 2021.

Hongyi Zhang, Moustapha Cisse, Yann N Dauphin, and David Lopez-Paz. mixup: Beyond empirical risk minimization. In *International Conference on Learning Representations*, 2018.

Qiming Zhang, Yufei Xu, Jing Zhang, and Dacheng Tao. Vitaev2: Vision transformer advanced by exploring inductive bias for image recognition and beyond. *arXiv preprint arXiv:2202.10108*, 2022.

Tianyuan Zhang and Zhanxing Zhu. Interpreting adversarially trained convolutional neural networks. In *International Conference on Machine Learning*, pp. 7502–7511. PMLR, 2019.

APPENDIX

A FURTHER INVESTIGATION ON SHORTCUT GENERATION

In Sec 3.2, we craft OPS by perturbing a fixed position to a fixed color target for each class. What if we only constrain one of these two properties? In other words, if perturbing a fixed position to different color targets, or perturbing different positions to a fixed color target, will a strong shortcut be created? With curiosity, we further explore these two properties individually.

We use OPS-Position and OPS-Color to represent the former and the latter setting. For OPS-Position, after finding the optimal position for each class via Algorithm 1, we perturb pixels at this position to random colors. For OPS-Color, we assign each class a predefined color (we add two colors since there are only 8 boundary colors) and perturb pixels at different positions to this color. Note that there might be many positions where the original color is already the same as the predefined color. We perturb the position where the original color is the furthest from the predefined color (measured by the l_2 norm) for each sample. As shown in Table A, the results indicate that if we only constrain one property, the resulting shortcuts will be harder to be captured. Besides, random perturbations at a fixed position can serve as a stronger shortcut than a fixed color at different positions.

Table A: One-Pixel Shortcut generated by different constraints. If perturbing a fixed position to different color targets or perturbing different positions to a fixed color target, the ability to degrade DNNs training will be less strong.

Training Data	Clean	OPS	OPS-Position	OPS-Color
Clean Test Acc.	94.01	15.56	46.22	85.34

B EXPLORATIONS ON $\mathcal{L}_2$ ADVERSARIAL TRAINING

In Sec 4.3, we have studied the effectiveness of different types of shortcuts under different types of training strategies, including l_∞ adversarial training and various data augmentations. For a more comprehensive exploration, we additionally evaluate them on l_2 adversarial training. Besides the commonly used setting ($\epsilon = 0.5$), we also try larger attack budgets, as shown in Table B.

Compared to l_∞, l_2 is proved to be a more efficient AT manner for alleviating OPS. Nevertheless, when the perturbation budget is not large enough, the network will still be affected by the shortcuts. If we further enlarge ϵ, it will hurt the clean test accuracy to a greater extent. As a local shortcut, OPS displays stronger inertia under l_2 AT, which can be viewed as a global data augmentation. As for EM, although generated by l_∞ perturbations, is still sensitive to l_2 AT. These results conform to our discussion about the properties of local&global shortcuts and local&global data augmentations in Sec 4.3.

Table B: ResNet-18 trained on different training data using l_2 adversarial training with different attack budgets.

Training Strategy	Training Data		
	Clean	OPS	EM
Standard	94.01	15.56	19.58
l_2 AT (ϵ=0.5)	87.68	43.26	71.00
l_2 AT (ϵ=1)	82.58	50.29	81.75
l_2 AT (ϵ=2)	73.45	73.70	74.51